National Marine
Fisheries Service
NOAA

Fishery Bulletin
established in 1881

Spencer F. Baird
First U.S. Commissioner
of Fisheries and founder
of *Fishery Bulletin*

Age, growth parameters, and reproductive characteristics of the sharpspine skate (*Okamejei acutispina*) in the East China Sea

Kojiro Hara
Keisuke Furumitsu
Atsuko Yamaguchi (contact author)

Email address for contact author: y-atsuko@nagasaki-u.ac.jp

Laboratory of Marine Zoology
Graduate School of Fisheries and Environmental Sciences
Nagasaki University
1-14 Bunkyo-machi
Nagasaki 852-8521, Japan

Abstract—The sharpspine skate (*Okamejei acutispina*) is a commercially exploited skate species in the East China Sea, and it is suspected that the population of this species in this region has declined due to fishing pressure and other factors. Nonetheless, information on its life history, which is essential for population assessment and management, is limited. We estimated its age, growth, maturity, and egg-laying season on the basis of data for 331 specimens captured in the East China Sea. Age was determined by counting translucent bands on vertebral centrum sections. Maximum total length (TL) and age were 448 mm and 10 years for females and 444 mm and 9 years for males. Among the 3 growth models applied to length-at-age data, the von Bertalanffy growth function provided the best fit for both sexes (females: theoretical asymptotic length [L_∞]=428 mm, growth coefficient [k]=0.30, and theoretical time a zero length [t_0]=−1.04 years; males: L_∞=422 mm, k=0.31, and t_0=−1.04 years). Size and age at 50% maturity were 380 mm TL and 4.60 years for females and 357 mm TL and 4.21 years for males. The monthly seasonal reproductive data, including egg case occurrence and oocyte maximum diameter, indicate a prolonged egg-laying season. Our findings indicate that the life history of the sharpspine skate in the East China Sea is characterized by a shorter lifespan, faster growth, and earlier age at maturity than many other skates globally.

Manuscript submitted 12 January 2024.
Manuscript accepted 16 April 2024.
Fish. Bull. 122:63–75 (2024).
Online publication date: 9 May 2024.
doi: 10.7755/FB.122.3.1

The sharpspine skate (*Okamejei acutispina*), a small skate belonging to the family Rajidae, inhabits sandy-muddy bottoms at depths of 20–175 m in the Northwest Pacific Ocean, from the waters of Japan south of the Niigata and Wakayama Prefectures to the East China Sea and waters of Taiwan (Yamada et al., 2007; Hatooka et al., 2013; Last et al., 2016).

In the East China Sea, located in both temperate and subtropical zones and bounded by China, South Korea, and Japan, the sharpspine skate is a predominant skate species, along with the polkadot skate (*Dipturus chinensis*), and is mainly found on the continental shelf edge (26–33°N) (Yamada et al., 2007; Hara et al., 2016). Data from a bottom-trawl survey conducted on the continental shelf of the central (approximately 126°30′E, 29°30′N) and northern (127°30′–128°00′E, 31°00′–32°30′N) East China Sea reveal that all skate specimens collected in the central waters were identified as sharpspine skate and that, in the northern waters, the sharpspine skate was the second-most collected skate species after the polkadot skate, accounting for 23% and 14% of all specimens by number and weight, respectively (Hara et al., 2016).

Skate species (Rajiformes) are captured (either as a targeted species or as bycatch) by commercial bottom trawlers of the countries that surround the East China Sea, in the sea and in adjacent waters, for human consumption (Baeck et al., 2011; Hara et al., 2014; Rigby et al., 2021). Commercial bottom trawlers from Japan directly target skates, and captured animals are then primarily processed into dried skate wings. Smaller skate species are generally of less economic value than larger ones; however, in this region, small-to-medium-sized skate species (up to 350–700 mm in total length [TL]), which are suitable for processing into dried skate wings, have considerable economic value and are targeted by bottom trawlers that operate from Japan (Hara et al., 2014). Consequently, in the East China Sea, the sharpspine skate is one of the main skate species targeted by bottom trawlers of Japan, in addition to the polkadot skate (Hara et al., 2014), and in other areas of the distribution of this species, the sharpspine skate is landed as a bycatch species (Rigby et al., 2021).

The continuous overexploitation by surrounding countries in the East China Sea over the past several decades

has led to a notable decline in the abundance of many demersal fish species (Yamada et al., 2007; Yamamoto and Nagasawa, 2015). Species-level catch data for skates have not been reported in Japan; however, for a reported category called *skates and rays*, annual landings by commercial bottom trawlers of Japan in the East China Sea have declined. In particular, there was a marked decline that began in the mid-1980s, from 3207 metric tons (t) in 1985 to 133 t in 2006 (data for 1993–2006 available at website; data for the full period from the 1980s to 2006 available in printed reports, MAFF[1]). Unfortunately, landings in subsequent years are unknown because, since 2007, catches of skates and rays have been included in the aggregated *other fish* category in government statistics. Although the decrease from the 1980s to 2006 in the annual catch of skates and rays appears to be consistent with the decreasing number of bottom trawlers from Japan operating in the region, results from an experimental trawl survey indicate a decline in skate populations, including those of the sharpspine skate (Yamada et al., 2007). Hence, the Ministry of the Environment, Japan, categorized the sharpspine skate as *near threatened* in 2017 (MEJ, 2017). Furthermore, in the IUCN Red List (Rigby et al., 2021), it is listed as *vulnerable*, on the basis of an estimated population reduction of 30–49% over the past 31 years due to fishing pressure.

Despite concerns about declining populations in the East China Sea, information on the life history of the sharpspine skate is extremely limited. Furthermore, published studies on its biology and ecology are scarce, even more than those on the polkadot skate, about which our recent studies have been published (Hara et al., 2018a, 2018b). In a previous study (Joung et al., 2011), the age and growth parameters of the sharpspine skate in the coastal waters of Taiwan, the southern limit of its range, were estimated; however, young of the year were not included in the estimation. Moreover, no published study has provided a detailed description of the overall life history characteristics of this species. To address this knowledge gap, we investigated, using specimens collected from the East China Sea, off southwestern Japan, the life history characteristics of the sharpspine skate, information about which is critical for accurate assessment of population status and conservation (Cailliet and Goldman, 2004). Specifically, we determined the age, growth parameters, and reproductive characteristics of the sharpspine skate, including its size and age at sexual maturity and egg-laying season.

Materials and methods

Sample collection and measurements

A total of 331 sharpspine skate (161 females and 170 males) were captured from April 2009 through November 2022 at depths of approximately 100–200 m in the central and northern East China Sea, off southwestern Japan (approximately between 27°30′N, 125°50′E and 32°20′N, 128°00′E). Skates were caught with bottom-trawl nets deployed from the commercial fishing vessels of the Yamada Suisan Co. Ltd.[2] (Nagasaki City, Japan) and the training ship of Nagasaki University (Hara et al., 2016, 2018a, 2018b). The TL (to the nearest 1 mm), disc width (DW, to the nearest 1 mm), body weight (BW, to the nearest 0.01 g), and sex of each individual were recorded in the laboratory. Although TL is a commonly used metric for measuring body size in skate life history studies, DW was used as a metric of size in a previous study on the age and growth of the sharpspine skate (Joung et al., 2011). Therefore, in our latest study that we describe herein, we employed DW as a metric, in addition to TL, for the purpose of comparison with size data from Joung et al. (2011).

A chi-square test was conducted to test whether the sex ratio was significantly different from 1:1. The relationship between TL and BW was calculated by using KyPlot, vers. 6.0 (KyensLab Inc., Tokyo, Japan). Analysis of covariance (ANCOVA), also done with KyPlot, was used to test for differences between the sexes in the relationship between TL and BW (both $\log_{10}$-transformed). Clasper length (to the nearest 0.01 mm), the distance from the posterior part of the cloaca to the tip of the clasper; oviducal gland width (to the nearest 0.01 mm); and the weights of the testes and ovaries (to the nearest 0.01 g) were recorded. Maturity stages were assigned on the basis of the scale of Hara et al. (2018a). The maximum diameter of oocytes (to the nearest 0.01 mm) in mature females was measured, and the presence or absence of egg cases in oviducts was recorded.

Age determination and growth estimation

For age determination, approximately 10 large vertebrae were extracted from the posterior portion of the abdominal cavity of specimen and immersed in 70% ethanol for 1–2 weeks. Each vertebral centrum was sectioned, following the procedure described by Hara et al. (2018a), with whetstones (#400–3000; Kai Corp. and Kai Industries Co. Ltd., Tokyo, Japan) (Fig. 1). The vertebral sections were air-dried for approximately 12 h, immersed in 100% ethanol, examined under a dissecting microscope by using reflected light (20× magnification), and then photographed by using a Nikon DS-Fi1 camera (Nikon Instruments Inc., Tokyo, Japan) attached to the microscope.

Age was determined by counting the translucent bands on the corpus calcareum (each band pair comprises a broad opaque band and a narrow translucent band). In this study, only fully completed translucent bands were counted as growth bands, and the translucent zones that were in the process of forming at the vertebral margins

[1] MAFF (Ministry of Agriculture, Forestry and Fisheries). 1980–2006. Annual statistics on fishery and aquaculture production. [In Japanese.] [Available from Prod. Mark. Consum. Stat. Div., MAFF. 1-2-1 Kasumigaseki, Chiyoda-ku, Tokyo 100-8950, Japan.]

[2] Mention of trade names or commercial companies is for identification purposes only and does not imply endorsement by the National Marine Fisheries Service, NOAA.

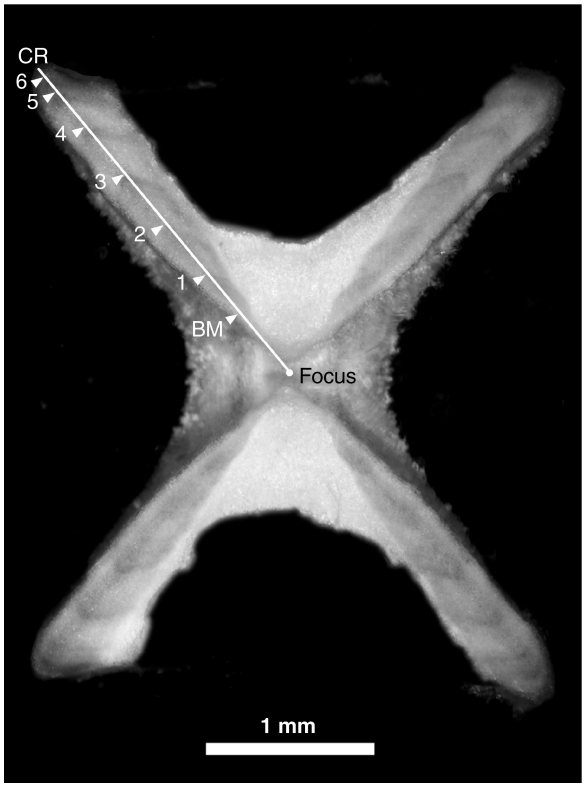

Figure 1

Photograph of the vertebral section from a female sharpspine skate (*Okamejei acutispina*) captured in the northern East China Sea on 20 August 2012. Arrows indicate the translucent bands (1–6). The estimated age of this specimen is 6 years, and its measured total length was 395 mm. CR=centrum radius; BM=birthmark.

(translucent margin) were not included in the age counts. Additionally, for each vertebral centrum, the first distinct band corresponding to a change of angle in the corpus calcareum was considered the birthmark and was not included in age determination (Sulikowski et al., 2007). Bands were counted twice by the same reader, without prior knowledge of specimen TL or sex. In cases for which the first and second counts differed, a third count was conducted. When the third count was consistent with either of the previous 2 counts, it was accepted; otherwise, the specimen was discarded. The reproducibility of the band count (age estimates) was evaluated by using average percentage error (APE) and Chang's coefficient of variation (CV) (Beamish and Fournier, 1981; Chang, 1982).

Centrum radius (CR) was measured from the focus to the distal margin. Distances from the focus to the translucent bands were measured at points along the margin of the corpus calcareum. Measured values of TL and DW were plotted against CR values, and an ANCOVA was performed on the $\log_{10}$-transformed data set to test for significant differences between sexes in the relationship between CR and TL and between CR and DW. The allometric function derived using the nonlinear least-squares procedure in KyPlot was used to describe the relationships between CR and TL and between CR and DW:

$$TL \text{ or } DW = uCR^{v}, \quad (1)$$

where u and v = constants.

To evaluate the periodicity of translucent band formation, marginal increment ratio (MIR) and edge analyses were performed. The MIR was calculated according to Hara et al. (2018a) as follows:

$$MIR = (CR - r_i) / (r_i - r_{i-1}), \quad (2)$$

where r_i = the radius of the last complete translucent band; and
r_{i-1} = the radius of the next-to-last complete translucent band.

Mean MIR was plotted against month, and the Kruskal–Wallis test (performed with KyPlot) was used to identify significant differences among months. Edge analysis was done on each vertebral section by determining whether the outer edge was translucent or opaque. The percentage of vertebrae with opaque or translucent margins was calculated monthly for all thin sections (Kume et al., 2008). Differences among months in the percentage of vertebrae with translucent margins were assessed by using Fisher's exact test (Fisher, 1922).

Back-calculation analysis was performed by using the body proportional hypothesis, a nonlinear method described by Francis (1990), because the samples lacked neonate individuals. For each individual, the TL and DW when the nth transparent band was formed (L_n) were back-calculated as follows:

$$L_n = (r_n / CR_c)^{v} L_c, \quad (3)$$

where r_n = the radius of the nth transparent band;
CR_c = the centrum radius at capture;
L_c = the specimen TL or DW at capture; and
v = a constant of the allometric CR–TL or CR–DW relationship.

To analyze the growth pattern, von Bertalanffy, Gompertz, and logistic growth models were fitted to back-calculated length-at-age data for each sex by using KyPlot, in which a quasi-Newton method is employed for nonlinear least-squares parameter estimation. Mature females with egg cases were observed throughout the sampling period, indicating a prolonged egg-laying season. Furthermore, the duration of embryonic development in the egg case is poorly known for this species. Therefore, we did not assign a theoretical birth date when estimating growth parameters of sharpspine skate to avoid the potential introduction of error and further uncertainty.

The von Bertalanffy, Gompertz, and logistic growth models were fitted by using Equations 4–6, respectively:

$$L_t = L_\infty(1 - \exp[-k(t - t_0)]); \quad (4)$$

$$L_t = L_\infty \exp(-\exp[-k(t - I)]); \text{ and} \quad (5)$$

$$L_t = \frac{L_\infty}{1+\exp\left(-k\left[t-I\right]\right)}, \quad (6)$$

where L_t = the calculated TL or DW at age t (in years);
L_∞ = the theoretical asymptotic length;
k = the growth coefficient;
t_0 = the theoretical time at zero length; and
I = the age at the curve's inflection point.

The goodness of fit of these 3 growth models was compared by using Akaike's information criterion (AIC) (Akaike, 1974). For the best-fit model, a likelihood-ratio test (Kimura, 1980) was performed to determine whether there was a significant difference in growth between sexes.

The maximum observed age based on vertebral-centrum analysis serves as an initial estimate of longevity, although this value may be underestimated if the population has been commercially exploited (Sulikowski et al., 2007). Therefore, theoretical longevity was estimated on the basis of the age at which 95% of L_∞ was reached, by using the growth coefficients from the von Bertalanffy, Gompertz, and logistic growth models in the following equation (Ricker, 1979):

$$5 \times \ln(2) \times k^{-1}. \quad (7)$$

Size and age at sexual maturity

Size at 50% maturity was estimated for each sex separately, by fitting a logistic model to both the maturity and length data through nonlinear least-squares parameter estimation in KyPlot (Furumitsu et al., 2019). The following logistic model was used:

$$Y = (1 + \exp[a + bX])^{-1}, \quad (7)$$

where Y = the proportion of mature individuals in each 10-mm size interval;
X = the TL (in millimeters); and
a and b = the empirical parameters.

Size at 50% maturity was calculated as $-ba^{-1}$. Age at 50% maturity was estimated directly for each sex from the age and maturity data of all aged individuals by using these methods.

Egg-laying season

The gonadosomatic index (GSI) for each mature individual was calculated by using the following formula:

$$GSI = \frac{Testis\ or\ ovary\ weight}{BW} \times 100. \quad (8)$$

To assess the reproductive cycle, monthly variation in mean GSI values was examined for each sex. The egg-laying season was estimated by examining the monthly variation in mean maximum diameter of oocytes and in the frequency of females with egg cases. Differences among months in the percentage of mature females with egg cases in their oviducts were assessed by using Fisher's exact test. Monthly differences in GSI values and in mean oocyte maximum diameter were tested by using one-way analysis of variance (ANOVA).

Results

Morphological measurements

Females (sample size [n]=161) ranged in size from 158 to 448 mm TL and from 115 to 319 mm DW, and males (n=170) ranged from 167 to 444 mm TL and from 134 to 295 mm DW. The distribution of total lengths of females and males is provided in Table 1. The overall sex ratio was not significantly different from 1:1 (chi-square test: χ^2=0.25, P>0.05). The relationship between TL and BW differed significantly between sexes (ANCOVA: F=30.5, P<0.001); therefore, this relationship was estimated separately for each sex as follows:

$$\text{Females: } BW = 6.06 \times 10^{-6} TL^{3.03} \text{ (coefficient of determination } [r^2]=0.93); \text{ and} \quad (9)$$

$$\text{Males: } BW = 2.23 \times 10^{-5} TL^{2.79} \ (r^2=0.93). \quad (10)$$

Age determination and growth estimation

The vertebrae from all 331 specimens were readable (APE=1.88%, CV=2.61%). The agreement between the 2 readings was 81.0%, and of those that did not agree, 95.2% differed by one band. Neither the relationship between CR and TL (ANCOVA: F=2.76, P>0.05) nor that between CR and DW (ANCOVA: F=1.65, P>0.05) was significantly different between the sexes. Therefore, the relationships were described for the pooled sexes as follows:

$$TL = 227 CR^{0.67} \ (r^2=0.94); \text{ and} \quad (11)$$

$$DW = 160 CR^{0.66} \ (r^2=0.92). \quad (12)$$

The strong correlations between CR and TL and between CR and DW indicate that centrum growth was proportional to body growth.

Table 1

Length distribution for female (sample size [n]=161) and male (n=170) sharpspine skates (*Okamejei acutispina*) sampled from the East China Sea between April 2009 and September 2022.

Total length class (mm)	n		
	Females	Males	Total
151–200	5	3	8
201–250	5	8	13
251–300	16	19	35
301–350	15	26	41
351–400	60	86	146
401–450	60	28	88
Total	161	170	331

The mean MIR differed significantly between months, with a distinct seasonal trend (Kruskal–Wallis test: χ^2=78.1, P<0.001). Specifically, the mean MIR value was highest in May and lowest in October (Fig. 2A). Edge analysis revealed that between March and August translucent margins appeared on the vertebral centra examined in this study, with the highest percentage of vertebrae with these margins observed in May (Fig. 2B); there was a significant difference in the frequency of translucent margins in different months (Fisher's exact test: P<0.001). Although no samples were available for July and for the period between December and February, a clear annual band formation pattern emerged, with translucent bands assumed to form once a year (i.e., from spring through summer).

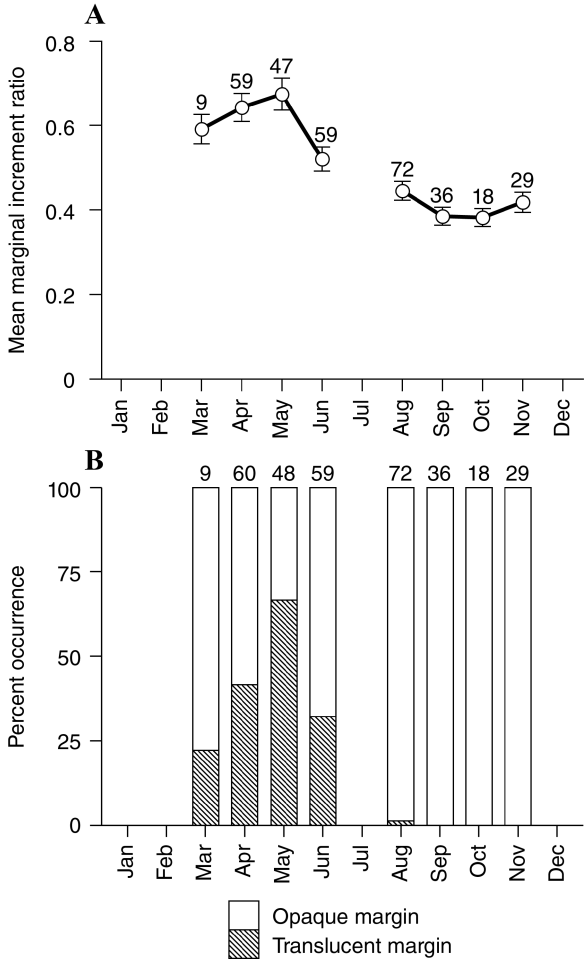

Figure 2

Monthly changes in (**A**) mean marginal increment ratio and (**B**) percent occurrence of opaque and translucent margins in the vertebral centra of sharpspine skates (*Okamejei acutispina*) sampled between April 2009 and November 2022 in the East China Sea. The error bars in panel A indicate standard errors of the mean. Numbers above circles and bars in panels A and B indicate sample sizes.

The mean back-calculated and observed lengths for each age class are presented in Table 2. For both sexes, the mean back-calculated lengths were close to the mean observed lengths at age for the class with ages ≥1 year. Meanwhile, the back-calculated lengths at birth (at age 0) were 45–67 mm smaller in TL and 33–54 mm smaller in DW than the observed lengths of young-of-the-year individuals; these size differences are attributed to the absence of neonates in our sample. The length at birth (based on TL) obtained through back-calculation analysis was 95–132 mm (mean: 113 mm) for females and 93–131 mm (mean: 114 mm) for males, values that are close to the previously reported TL of approximately 110 mm (Last et al., 2016). The back-calculated length (based on TL) at formation of the first growth band was 171–233 mm (mean: 201 mm) for females and 162–233 mm (mean: 202 mm) for males; Lee's phenomenon (Ricker, 1975) was not evident.

The growth parameters of the von Bertalanffy, Gompertz, and logistic growth models estimated from back-calculated length-at-age data are presented in Table 3. Among these growth models, the von Bertalanffy growth function had the lowest AIC for both sexes and was chosen as the best-fit model, regardless of whether TL or DW was used as the size metric (Table 3). The likelihood-ratio test revealed that there were significant differences in growth patterns between the sexes, when either TL (χ^2=13.2, df=3, P<0.01) or DW (χ^2=253.2, df=3, P<0.001) was used as the size metric. Results from likelihood-ratio tests for each parameter indicate significant differences between the sexes for all parameters, regardless of whether TL (L_∞: χ^2=7.1, df=1, P<0.01; k: χ^2=10.3, df=1, P<0.01; and t_0: χ^2=13.0, df=1, P<0.001) or DW (L_∞: χ^2=112.3, df=1, P<0.001; k: χ^2=241.5, df=1, P<0.001; and t_0: χ^2=252.7, df=1, P<0.001) was used as the size metric.

The von Bertalanffy growth function revealed that both sexes reached >80% of L_∞ at 5 years of age (Fig. 3). The observed maximum age was 10 years (TL: 402–448 mm; DW: 280–319 mm) for females and 9 years (TL: 412–444 mm; DW: 262–295 mm) for males. The theoretical longevity predicted by using the von Bertalanffy growth function was 11.5 years for females and 11.2 years for males, based on TL, and it was 11.3 years for females and 10.7 years for males, based on DW, estimates that are slightly higher than the maximum observed age. In contrast, the predictions of theoretical longevity from the Gompertz and logistic growth models were markedly lower than the maximum observed age for both sexes (Table 3).

Size and age at sexual maturity

Oviducal gland width increased abruptly when TL was approximately 320 mm, a pattern consistent with the observations of premature females, and oviducal gland growth slowed after sexual maturity (Fig. 4A). Clasper length increased abruptly in males with TLs >330 mm and slowed after sexual maturity (Fig. 4B).

The smallest sexually mature female and male were 366 and 355 mm TL, respectively. All females with TLs >389 mm and males with TLs >390 mm were mature. Size

Table 2

Mean back-calculated and observed total length (in millimeters) and disc width (in millimeters) at each age for female and male sharpspine skates (*Okamejei acutispina*) captured from April 2009 through November 2022 in the East China Sea. SD=standard deviation; *n*=sample size.

Sex and size measurement	Age (years)										
	0	1	2	3	4	5	6	7	8	9	10
Female											
Back-calculated											
Total length	113	201	256	298	332	358	377	391	398	408	420
SD	6.1	12.7	14.0	15.0	15.9	16.8	17.0	15.9	13.4	12.0	11.9
Disc width	82	144	182	212	235	254	267	275	282	286	295
SD	4.7	9.4	10.8	11.8	12.3	13.4	13.1	11.8	10.6	10.6	10.8
n	161	160	152	136	124	100	80	53	32	19	8
Observed											
Total length	158	202	270	327	362	386	398	412	410	414	426
SD		14.4	14.5	19.3	14.6	11.5	14.1	11.4	13.9	12.8	13.7
Disc width	115	143	190	232	255	274	283	287	293	290	299
SD		9.5	10.8	17.9	12.3	10.7	10.5	11.4	7.3	10.8	12.0
n	1	8	16	12	24	20	27	21	13	11	8
Male											
Back-calculated											
Total length	114	202	257	298	332	357	375	388	402	418	
SD	5.9	11.5	13.3	14.3	15.6	15.3	12.8	11.2	10.0	12.9	
Disc width	80	141	178	205	227	244	255	264	270	279	
SD	4.2	8.2	9.5	10.2	11.2	11.0	10.0	9.3	9.4	7.2	
n	170	169	161	144	125	101	70	42	10	3	
Observed											
Total length	181	219	269	317	354	381	392	398	406	426	
SD		28.1	17.0	17.2	16.4	14.5	10.6	11.6	9.3	16.4	
Disc width	134	155	190	221	244	260	268	271	273	284	
SD		20.6	13.2	12.1	11.0	9.0	8.7	9.2	11.3	9.5	
n	1	8	17	19	24	31	28	32	7	3	

at 50% sexual maturity was 380 mm TL for females and 357 mm TL for males (Fig. 4C).

The youngest mature individuals of both sexes were 4 years old. For both sexes, all individuals with assigned ages of 6 years or older were sexually mature. The age at 50% sexual maturity was 4.60 years for females and 4.21 years for males (Fig. 4D).

Egg-laying season

Mature females and males appeared in all months sampled (Fig. 5, A and B). There were no significant differences in GSI values among months for either females (one-way ANOVA: F=1.26, P>0.05) or males (one-way ANOVA: F=1.80, P>0.05) (Fig. 5, C and D). Maximum diameter of oocytes was not significantly different among months (one-way ANOVA: F=1.37, P>0.05), and all the mature females had yellow vitellogenic oocytes ≥15 mm in diameter (Fig. 5E).

Of the 98 mature females, 54 skates (55.1%) were carrying egg cases in their oviducts. Of these females, 33 individuals had an egg case in both the right and left oviducts, and 21 individuals had an egg case in only one of the oviducts. Mature females with egg cases were observed in all the collection months, indicating that the sharpspine skate has a prolonged egg-laying season with a span of at least March–November (Fig. 5F). The frequency of mature females carrying egg cases was the highest in October (100%), high in May (85.7%), and the lowest in August (42.9%), although these differences between months were not statistically significant (Fisher's exact test: P>0.05).

Discussion

Our aging method achieved optimal precision and reproducibility in age estimation, with an APE and a CV that were markedly lower than the thresholds for acceptance of 5.5% APE and 7.6% CV suggested by Campana (2001).

Owing to the lack of samples of sharpspine skate collected in July and in the period December–February, we were unable to fully validate the annual band formation of sharpspine skate in the East China Sea. However, the clear periodicity of translucent band formation detected through both the MIR and edge analyses indicates that a single translucent band is likely to form annually between spring and summer. Hence, the time required from hatching to the formation of the first growth band may vary

Table 3

Comparison of estimated growth parameters and goodness of fit for the von Bertalanffy, Gompertz, and logistic growth models fitted to back-calculated length-at-age data for female and male sharpspine skates (*Okamejei acutispina*) sampled from April 2009 through November 2022 in the East China Sea. The parameters are theoretical asymptotic length (L_∞), with length in total length or disc width; growth coefficient (k); theoretical time at zero length (t_0); and age at the curve inflection point (I). The 95% confidence intervals for parameter estimates are provided in parentheses. Theoretical longevity was estimated as the age at which 95% of L_∞ was reached: $5\times\ln(2)\times k^{-1}$. Akaike's information criterion (AIC) values were used to compare the goodness of fit of the 3 growth models. The sample sizes (n) for back-calculated length-at-age data are also provided.

	von Bertalanffy		Gompertz		Logistic	
Parameter	Females	Males	Females	Males	Females	Males
Total length						
L_∞ (mm)	428 (423–432)	422 (418–427)	405 (402–408)	396 (392–399)	394 (391–397)	383 (380–386)
k (years^{-1})	0.30 (0.29–0.31)	0.31 (0.30–0.32)	0.47 (0.46–0.49)	0.50 (0.49–0.51)	0.65 (0.63–0.67)	0.69 (0.68–0.71)
t_0	−1.04 (−1.08 to −1.01)	−1.04 (−1.07 to −1.00)				
I			0.40 (0.37–0.43)	0.35 (0.32–0.37)	1.15 (1.11–1.18)	1.04 (1.01–1.07)
n	1025	995	1025	995	1025	995
Longevity	11.5	11.2	7.3	6.9	5.3	5.0
AIC	8336	7911	8501	8087	8713	8299
Disc width						
L_∞ (mm)	300 (297–303)	283 (280–286)	285 (283–287)	267 (265–270)	278 (275–280)	259 (257–261)
k (years^{-1})	0.31 (0.30–0.32)	0.32 (0.31–0.34)	0.48 (0.46–0.49)	0.51 (0.50–0.53)	0.65 (0.63–0.67)	0.70 (0.68–0.72)
t_0	−1.06 (−1.11 to −1.02)	−1.05 (−1.09 to −1.01)				
I			0.35 (0.32–0.38)	0.27 (0.25–0.30)	1.09 (1.06–1.13)	0.95 (0.92–0.98)
n	1025	995	1025	995	1025	995
AIC	7801	7264	7930	7409	8104	7593
Longevity	11.3	10.7	7.3	6.8	5.3	5.0

widely among individuals, as the sharpspine skate in the East China Sea has a continuous egg-laying season that has a span of at least March–November. Moreover, the back-calculated lengths at age 1 (based on TL) varied by up to 1.39 times for females and 1.41 times for males. The variation in these lengths may be at least partially attributable to differences in birth dates among individuals. However, no vertebrae were observed with the first growth band formed very close to the birthmark, indicating that individuals hatched just before the period of growth band formation may form their first growth band the following year, rather than within the same year.

Consistent with our findings, Joung et al. (2011) reported that, for sharpspine skate from the coastal waters of Taiwan, translucent margins were most frequently observed in May. Therefore, the results of both studies indicate a similar timing for formation of translucent bands for this species in both the East China Sea and Taiwan. Similarly, Yamaguchi et al. (1998) found that, for the starspotted smooth-hound (*Mustelus manazo*), the timing of band formation did not differ among 5 geographically distant areas in Japan and Taiwan; they proposed that growth band formation may not be caused by reproduction and water temperature but may be influenced by factors other than a change in location.

The von Bertalanffy growth function has traditionally been used in modeling fish growth, including for elasmobranch species (Cailliet et al., 2006). However, the results of an increasing number of studies indicate that the Gompertz or logistic growth models provide better fits for length-at-age data than the von Bertalanffy growth function, especially for skates and rays (Jacobsen and Bennett, 2011; Porcu et al., 2020; Bellodi et al., 2021). Joung et al. (2011) showed that the logistic growth model is the best fit for describing the growth patterns of sharpspine skate in Taiwan. In our study, however, on the basis of AIC values, the von Bertalanffy growth function provided the best fit for describing the growth pattern of sharpspine skate in the East China Sea. For both sexes, the von Bertalanffy growth function predicted an L_∞ that approximates the observed maximum length, whereas the predictions of the Gompertz and logistic growth models were much smaller.

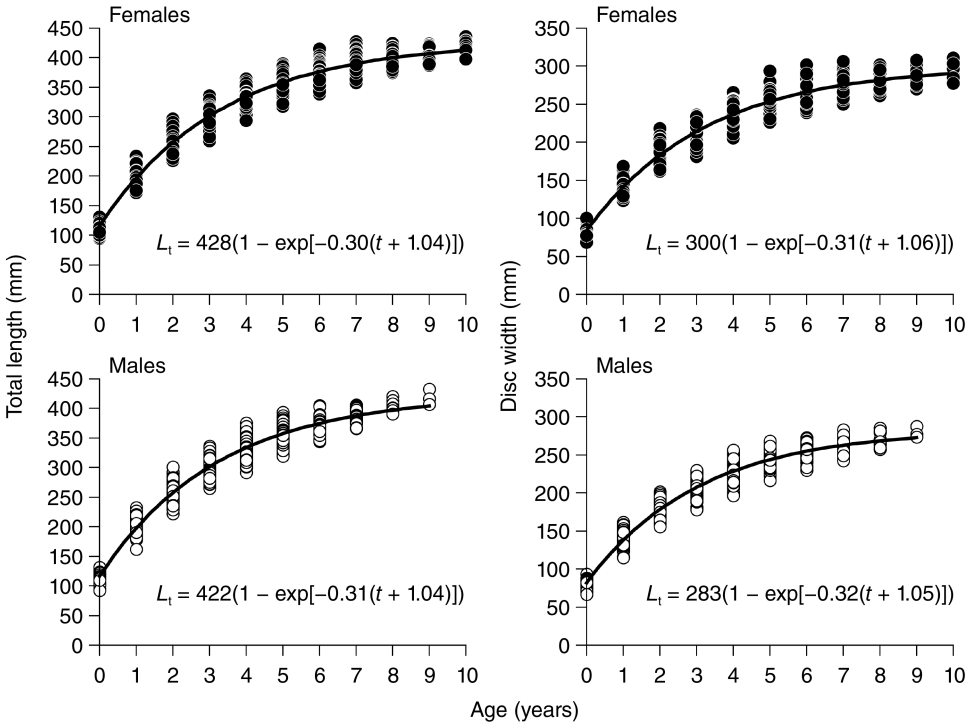

Figure 3

von Bertalanffy growth curves fitted to back-calculated length-at-age data for female and male sharpspine skates (*Okamejei acutispina*). Data used in the growth model are back-calculated total lengths and disc widths from specimens captured from April 2009 through November 2022 in the East China Sea. The equation for calculated length at age t (L_t) is given under each curve.

Additionally, the theoretical longevity derived from the k values estimated with the Gompertz and logistic growth models was much less than the observed maximum age for females and males, and therefore, was not biologically realistic. In summary, the von Bertalanffy growth function provided the most biologically reasonable parameter estimates for both sexes.

Goodness of fit for growth models can be influenced by several factors, including data quality, sample size, and dispersion of data across size classes (Cailliet et al., 2006). The logistic growth model may provide a better fit than the von Bertalanffy growth function if the length distribution is skewed toward larger sizes (Bellodi et al., 2022). Although the samples both in our study presented herein and in that by Joung et al. (2011) were biased toward larger (or older) individuals, our use of back-calculation effectively increased the number of length-at-age data points for younger (smaller) individuals for the growth models. This increase in data points for younger individuals might have contributed to the discrepancy in the best-fit model between this study and that of Joung et al. (2011). The use of back-calculation in our study may also have contributed to the description of the biologically reasonable growth pattern of the sharpspine skate, given that the length at age 0 from the von Bertalanffy growth function (116 mm TL for females and 115 mm TL for males) approximated the previously reported length at birth, despite the lack of neonates in our sample.

The maximum size in DW of sharpspine skate in Taiwan was 338 mm for females and 289 mm for males (Joung et al., 2011), indicating that females from the East China Sea attain a slightly smaller size than those from Taiwan and that males attain sizes that are similar between locations. The maximum ages observed in our study were 10 years for females and 9 years for males; each of these ages is 1 year younger than the maximum age reported for each sex of this species in Taiwan (Joung et al., 2011).

For all 3 growth models, the growth rates (k values) were markedly higher in our study than in that by Joung et al. (2011); for the von Bertalanffy growth function fitted to DW data, k was 0.31 for females and 0.32 for males in our study but 0.15 for females and 0.17 for males in that by Joung et al. (2011). Indeed, for nearly all age groups, the DW at age estimated from the von Bertalanffy growth function was larger in our study than in that by Joung et al. (2011) for both sexes. Geographic variation in estimates of age and growth parameters has often been reported for elasmobranchs, including several skate species (Yamaguchi et al., 1998; Frisk and Miller, 2006; Licandeo and Cerna, 2007; Bellodi et al., 2022). These geographic variations may be caused by several factors, including differences in environmental conditions, food availability, and fishing-related

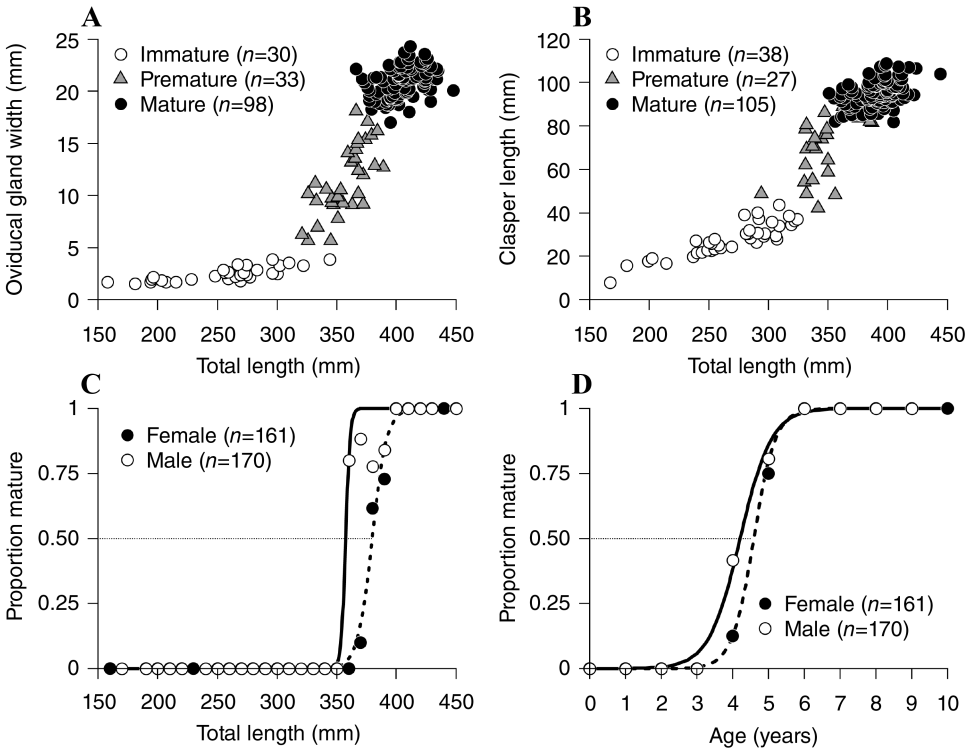

Figure 4

Maturation of female and male sharpspine skates (*Okamejei acutispina*) sampled between April 2009 and November 2022 in the East China Sea. The top panels show the relationship between total length and (**A**) oviducal gland width for females or (**B**) clasper length for males. The bottom panels show the (**C**) size and (**D**) age at maturity for females (dashed line) and males (solid line). The horizontal dotted line in each bottom panel indicates the size at 50% maturity. *n*=sample size.

mortality and could reflect the existence of separate stocks (Yamaguchi, 2002). Alternatively, such variations may also be due to other factors, such as sample bias and differences in readers, reading precision, preparation techniques, and growth modeling approaches (Cailliet et al., 1990; Carbonara et al., 2020). Therefore, evaluating whether the large differences between the East China Sea and Taiwan in observed growth patterns truly reflect geographic differences or result from methodological issues requires involving the same readers making comparisons using the same methods to minimize error, as was demonstrated by Yamaguchi et al. (1998).

Based on life history data (Caltabellotta et al., 2019) and the range of life history variation (Frisk, 2010; Ebert et al., 2017) for 28 skate species, the maximum observed age varies greatly among species, from 6 years for the Rio skate (*Rioraja agassizii*) to 37 years for the whitebrow skate (*Bathyraja minispinosa*). Frisk (2010) calculated the mean observed maximum age of skates, using data from 14 skate species available at the time, as 17.5 years for females and 17.3 years for males. In our study, the maximum observed ages for both sexes of sharpspine skate were relatively low, similar to those reported by Joung et al. (2011), although they were within the range reported for skates. The maximum observed age has also been reported to be relatively low for several other small-sized skates, including the roundel skate (*Rostroraja texana*), the brown ray (*Raja miraletus*), and the speckled ray (*Raja polystigma*), with maximum observed ages ranging from 9 to11 years for females and from 7 to 8 years for males (Sulikowski et al., 2007; Kadri et al., 2012; Porcu et al., 2020). Because the sharpspine skate is among the smallest skate species for which age and growth data are available, the results of our study and of that by Joung et al. (2011) are consistent with the general trend that smaller skate species reach a lower maximum age than larger species (Sulikowski et al., 2007).

For both sexes of sharpspine skate in the East China Sea, k was considerably higher than the mean k value for skates (1.20 for females and 1.40 for males) calculated by Frisk (2010) on the basis of published estimates for parameters of the von Bertalanffy growth function. The growth rates derived with the von Bertalanffy growth function for skate species range from 0.02 for the whitebrow skate to 0.34 for the Sydney skate (*Dentiraja australis*), with very few species (such as the sharpspine skate in this study) exceeding 0.30 (Gallagher et al., 2005; Frisk, 2010; Ebert et al., 2017; Reis and Figueira, 2020). Estimates made

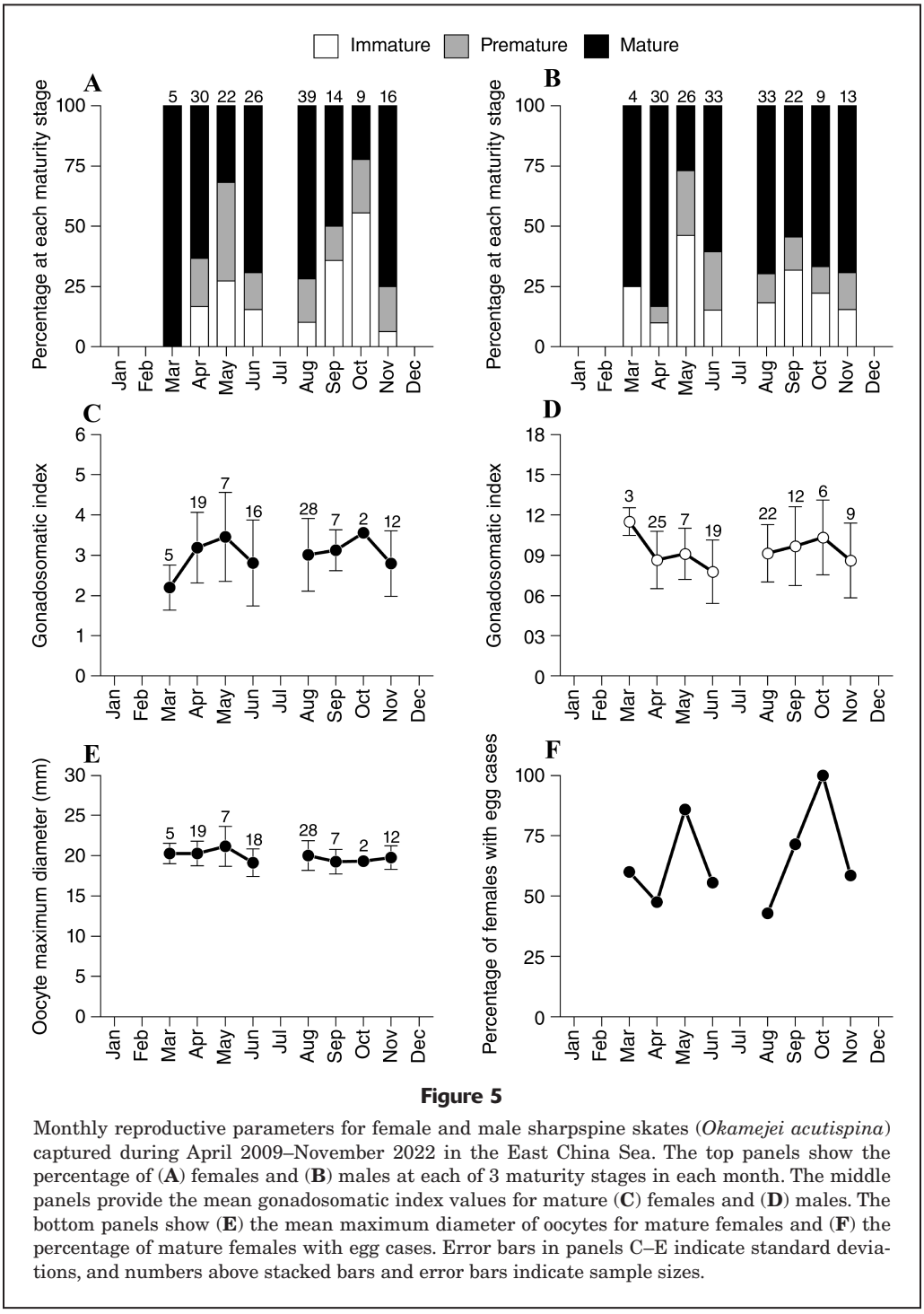

Figure 5

Monthly reproductive parameters for female and male sharpspine skates (*Okamejei acutispina*) captured during April 2009–November 2022 in the East China Sea. The top panels show the percentage of (**A**) females and (**B**) males at each of 3 maturity stages in each month. The middle panels provide the mean gonadosomatic index values for mature (**C**) females and (**D**) males. The bottom panels show (**E**) the mean maximum diameter of oocytes for mature females and (**F**) the percentage of mature females with egg cases. Error bars in panels C–E indicate standard deviations, and numbers above stacked bars and error bars indicate sample sizes.

with the von Bertalanffy growth function in our study indicate that both sexes of sharpspine skate in the East China Sea grow rapidly up to 5 years of age, reaching approximately 360 mm TL, after which point growth slows. These findings reveal that sharpspine skate in the East China Sea grow faster than those in Taiwan and most other skate species for which age and growth data are available, with the greater part of the growth occurring during the first half of their life.

In our study, estimated size at 50% maturity was 84.8% and 80.0% of the maximum observed length for this species for females and males, respectively, falling within the typical range (75–90%) reported for skates (Ebert et al., 2008). Although the maximum observed lengths were nearly the same for both sexes, the size at 50% maturity was approximately 25 mm TL larger for females than for males, indicating slight sexual dimorphism in size at maturity. Female elasmobranchs typically mature

at a larger size than males. Nonetheless, in skates, the occurrence of sexual dimorphism in size at maturity varies among species. For instance, for the roundel skate (Sulikowski et al., 2007), brown ray (Kadri et al., 2012), and white skate (*Rostroraja alba*) (Ebert et al., 2008), females mature at a slightly larger size than males, consistent with our latest findings for the sharpspine skate. For the bigthorn skate (*Rajella barnardi*), in contrast, the sexes mature at approximately the same size (Ebert et al., 2008). Moreover, for some species, such as the zipper sandskate (*Psammobatis extenta*) (Braccini and Chiaramonte, 2005) and the African softnose skate (*Bathyraja smithii*) (Ebert et al., 2008), males mature at a slightly larger size than females.

For both sexes in our study, the youngest mature sharpspine skate was estimated to be 4 years old, and the age at 50% maturity corresponded to 46.0% of the maximum observed age for females and 46.8% of this age for males. Among the elasmobranchs, which are generally slow to mature, skates tend to mature particularly slowly (Frisk, 2010; Hara et al., 2018a). According to Frisk (2010), the mean age at 50% maturity for skate species is 10.1 years for females and 9.1 years for males, that is, approximately 64% of the maximum age for females and approximately 60% of this age for males. Therefore, sharpspine skate in the East China Sea appear to have a lower age at maturity than many other skate species, maturing very early in its life span.

In the East China Sea, the sharpspine skate occurs sympatrically with several other skate species, such as the polkadot skate, the bigeye skate (*Okamejei meerdervoortii*), and the acutenose skate (*Dipturus tengu*) (Hara et al., 2016), but their species-specific biological information is very limited, with comparable life history data available only for the polkadot skate (Hara et al., 2018a). Sharpspine skate in our latest study had a maximum age 5 years lower for females and 4 years lower for males, compared with that of the polkadot skate, and growth rates of sharpspine skate were much higher for both sexes than for those of the polkadot skate (0.30 versus 0.10 for females and 0.31 versus 0.11 for males) (Hara et al., 2018a). In addition, the 50% age at maturity of female and male sharpspine skate was approximately half that of polkadot skate (Hara et al., 2018a). Given that these species coexist and presumably occupy similar ecological niches and are fished together, the population dynamics of the sharpspine skate and the polkadot skate likely interact. Therefore, it is appropriate to assess the population status and establish fisheries management for each species separately.

Prior to this study, there was a lack of reliable information on the egg-laying season of the sharpspine skate. The lack of samples for the period December–February and for July prevented us from determining the full extent of its egg-laying cycle. However, on the basis of our results, we do have evidence that the egg-laying season of this species spans at least from March through November, as there was no significant difference in the maximum diameter of oocytes in different months and mature females with egg cases were found in all the months sampled. Because measuring egg-laying rates in the wild for oviparous elasmobranchs like skates is challenging (Frisk, 2010), the annual fecundity could not be estimated in this study. Overall, more than half of the mature females were carrying egg cases, indicating that they repeatedly lay egg cases at short intervals. The frequency of females with egg cases was high in May and November but was not significantly different among months.

We were unable to draw strong conclusions regarding egg-laying seasonality because, for some months (especially in November), few mature females were obtained. However, given the lack of a significant difference in monthly GSI values for mature females, the 2 peaks that were observed in the percentage of females with egg cases may not reflect egg-laying seasonality. Year-round egg-laying, with or without seasonal peaks, has been reported for many skate species, such as the thorny skate (*Amblyraja radiata*), little skate (*Leucoraja erinacea*), brown ray, and polkadot skate (Sulikowski et al., 2005; Palm et al., 2011; Kadri et al., 2012; Hara et al., 2018a). Additional sampling in December–February, in July, and in the months when few mature females were collected is needed to fully determine the annual egg-laying cycle of the sharpspine skate and to verify whether this species also lays egg cases throughout the year.

The similarity among months in the GSI for mature males indicates that males of this species may be capable of reproducing continuously. In male elasmobranchs, however, temporal variation in GSI values does not always synchronize with spermatogenesis (Sulikowski et al., 2005). Furthermore, the females of some skate species can store sperm in the oviducal glands (Luer and Gilbert, 1985; Soto-López et al., 2021). Therefore, histological examination of male testes is necessary to fully elucidate the reproductive cycle of the sharpspine skate.

Conclusions

The results of this study provide comprehensive information on the life history characteristics of the sharpspine skate in the East China Sea. Our findings reveal that, although the sharpspine skate in the East China Sea has a prolonged egg-laying season, as is typical for skates, it is short-lived, grows faster, and matures much earlier than many other skate species, including the sympatric polkadot skate. These unique life history traits of the sharpspine skate in the East China Sea have important implications for its population assessment and sustainable management as a fishery resource, and they highlight the need for species-specific life history investigations and population monitoring for skates in this region, many of which are targeted by bottom trawlers. Finally, because the growth pattern of sharpspine skate in the East China Sea estimated in this study is substantially different from that of the same species in Taiwan, further study is recommended to verify the existence of geographic differences in life history traits and the possible existence of distinct regional populations.

Resumen

La raya picuda (*Okamejei acutispina*) es una especie de raya explotada comercialmente en el Mar Oriental de China, y se sospecha que la población de esta especie en esta región ha disminuido debido a la presión pesquera y a otros factores. Sin embargo, la información sobre su ciclo vital, esencial para la evaluación y manejo de la población, es limitada. Estimamos la edad, crecimiento, madurez y su época de desove a partir de los datos de 331 ejemplares capturados en el Mar Oriental de China. La edad se determinó contando las bandas translúcidas en las secciones del centro vertebral. La máxima longitud total (LT) y edad fue 448 mm y 10 años para hembras y 444 mm y 9 años para machos. Entre los 3 modelos de crecimiento aplicados a los datos de longitud a la edad, la función de crecimiento de von Bertalanffy proporcionó el mejor ajuste para ambos sexos (hembras: longitud asintótica teórica [L_∞]=428 mm, coeficiente de crecimiento [k]=0.30 y tiempo teórico a longitud cero [t_0]=−1.04 años; machos: L_∞=422 mm, k=0.31 y t_0=−1.04 años). La talla y la edad al 50% de madurez fueron 380 mm LT y 4.60 años para las hembras y 357 mm LT y 4.21 años para los machos. Los datos reproductivos estacionales mensuales, incluyendo la aparición de huevos y el diámetro máximo del oocitos, indican una prolongada temporada de desove. Nuestros hallazgos indican que la historia de vida de la raya de espina afilada en el Mar Oriental de China se caracteriza por una vida más corta, un crecimiento más rápido y una edad de madurez menor que la de muchas otras rayas del mundo.

Acknowledgments

We are grateful to T. Ozaki and S. Takase (Yamada Suisan Co. Ltd.) and the officers and crew of the Nagasaki University training ship for their help with sample collection. This study was financially supported by a Grant-in-Aid for Scientific Research (B) (19H02977, 23H02237) from the Japan Society for the Promotion of Science and by the Environment Research and Technology Development Fund (1-2203) of the Environmental Restoration and Conservation Agency of Japan.

Literature cited

Akaike, H.
1974. A new look at the statistical model identification. IEEE Trans. Autom. Control 19:716–723. Crossref

Baeck, G. W., C.-I. Park, H. C. Choi, S.-H. Huh, and J. M. Park.
2011. Feeding habits of ocellate spot skate, *Okamejei kenojei* (Müller & Henle, 1841), in coastal waters of Taean, Korea. J. Appl. Ichthyol. 27:1079–1085. Crossref

Beamish, R. J., and D. A. Fournier.
1981. A method for comparing the precision of a set of age determinations. Can. J. Fish. Aquat. Sci. 38:982–983. Crossref

Bellodi, A., A. Mulas, P. Carbonara, A. Cau, D. Cuccu, M. F. Marongiu, V. Mura, P. Pesci, W. Zupa, C. Porcu, et al.
2021. New insights into life-history traits of Mediterranean electric rays (Torpediniformes: Torpedinidae) as a contribution to their conservation. Zoology 146:125922. Crossref

Bellodi, A., A. Massaro, W. Zupa, M. Donnaloia, M. C. Follesa, A. Ligas, A. Mulas, M. Palmisano, and P. Carbonara.
2022. Assessing thornback ray growth pattern in different areas of Western-Central Mediterranean Sea through a Multimodel Inference analysis. J. Sea Res. 179:102141. Crossref

Braccini, J. M., and G. E. Chiaramonte.
2005. Reproductive biology of *Psammobatis extenta*. J. Fish Biol. 61:272–288. Crossref

Cailliet, G. M., and K. J. Goldman.
2004. Age determination and validation in chondrichthyan fishes. *In* Biology of sharks and their relatives (J. Carrier, J. A. Musick, and M. Heithaus, eds.), p. 399–447. CRC Press, Boca Raton, FL.

Cailliet, G. M., K. G. Yudin, S. Tanaka, and T. Taniuchi.
1990. Growth characteristics of two populations of *Mustelus manazo* from Japan based upon cross-readings of vertebral bands. *In* Elasmobranchs as living resources: advances in the biology, ecology, systematics, and the status of the fisheries (H. L. Pratt, Jr., S. H. Gruber, and T. Taniuchi, eds.), p. 167–176. NOAA Tech. Rep. NMFS 90.

Cailliet, G. M., W. D. Smith, H. F. Mollet, and K. J. Goldman.
2006. Age and growth studies of chondrichthyan fishes: the need for consistency in terminology, verification, validation, and growth function fitting. Environ. Biol. Fishes 77:211–228. Crossref

Caltabellotta, F. P., F. M. Silva, F. S. Motta, and O. B. F. Gadig.
2019. Age and growth of the threatened endemic skate *Rioraja agassizii* (Chondrichthyes, Arhynchobatidae) in the western South Atlantic. Mar. Freshw. Res. 70:84–92. Crossref

Campana, S. E.
2001. Accuracy, precision and quality control in age determination, including a review of the use and abuse of age validation methods. J. Fish Biol. 59:197–242. Crossref

Carbonara, P., A. Bellodi, M. Palmisano, A. Mulas, C. Porcu, W. Zupa, M. Donnaloia, R. Carlucci, L. Sion, and M. C. Follesa.
2020. Growth and age validation of the thornback ray (*Raja clavata* Linnaeus, 1758) in the South Adriatic Sea (central Mediterranean). Front. Mar. Sci. 7:586094. Crossref

Chang, W. Y. B.
1982. A statistical method for evaluating the reproducibility of age determination. Can. J. Fish. Aquat. Sci. 39:1208–1210. Crossref

Ebert, D. A., L. J. V. Compagno, and P. D. Cowley.
2008. Aspects of the reproductive biology of skates (Chondrichthyes: Rajiformes: Rajoidei) from southern Africa. ICES J. Mar. Sci. 65:81–102. Crossref

Ebert, D. A., J. S. Bigman, and J. M. Lawson.
2017. Biodiversity, life history, and conservation of northeastern Pacific chondrichthyans. *In* Northeast Pacific shark biology, research and conservation, part A. Advances in Marine Biology, vol. 77 (S. E. Larson, and D. Lowry, eds.), p. 9–78. Acad. Press, London.

Fisher, R. A.
1922. On the interpretation of χ^2 from contingency tables, and the calculation of P. J. R. Stat. Soc. 85:87–94.

Francis, R. I. C. C.
1990. Back-calculation of fish length: a critical review. J. Fish Biol. 36:883–902. Crossref

Frisk, M. G.
2010. Life history strategies of batoids. *In* Sharks and their relatives 2: biodiversity, adaptive physiology, and conservation (J. C. Carrier, J. A. Musick, and M. Heithaus, eds.), p. 283–316. CRC Press, Boca Raton, FL.

Frisk, M. G., and T. J. Miller.
2006. Age, growth, and latitudinal patterns of two Rajidae species in the northwestern Atlantic: little skate (*Leucoraja*

erinacea) and winter skate (*Leucoraja ocellata*). Can. J. Fish. Aquat. Sci. 63:1078–1091. Crossref

Furumitsu, K., J. T. Wyffels, and A. Yamaguchi.
2019. Reproduction and embryonic development of the red stingray *Hemitrygon akajei* from Ariake Bay, Japan. Ichthyol. Res. 66:419–436. Crossref

Gallagher, M. J., C. P. Nolan, and F. Jeal.
2005. Age, growth and maturity of the commercial ray species from the Irish Sea. J. Northwest Atl. Fish. Sci. 35:47–66. Crossref

Hara, K., K. Furumitsu, and A. Yamaguchi.
2014. Record of a Korean skate, *Hongeo koreana* (Jeong and Nakabo, 1997) from off the Goto Islands. Rep. Japan. Soc. Elasmobranch Stud. 50:21–26. [In Japanese.]

Hara, K., K. Furumitsu, T. Aoshima, Y. Morii, N. Yamawaki, N. Kusumoto, H. Kanehara, and A. Yamaguchi.
2016. Species composition of skates (Rajiformes: Rajoidei) collected in the East China Sea, during the cruise of the T/S *Nagasaki-Maru*. Rep. Japan. Soc. Elasmobranch Stud. 52:5–11. [In Japanese.]

Hara, K., K. Furumitsu, T. Aoshima, H. Kanehara, and A. Yamaguchi.
2018a. Age, growth, and age at sexual maturity of the commercially landed skate species, *Dipturus chinensis* (Basilewsky, 1855), in the northern East China Sea. J. Appl. Ichthyol. 34:66–72. Crossref

Hara, K., K. Furumitsu, and A. Yamaguchi.
2018b. Dietary habits of the polkadot skate *Dipturus chinensis* in the East China Sea. Ichthyol. Res. 65:363–373. Crossref

Hatooka, K., U. Yamada, M. Aizawa, A. Yamaguchi, and N. Yagishita.
2013. Rajidae. *In* Fishes of Japan with pictorial keys to the species, 3rd ed. (T. Nakabo, ed.), p. 205–216. Tokai Univ. Press, Hadano, Japan. [In Japanese.]

Jacobsen, I. P., and M. B. Bennett.
2011. Life history of the blackspotted whipray *Himantura astra*. J. Fish Biol. 78:1249–1268. Crossref

Joung, S.-J., P.-H. Lee, K.-M. Liu, and Y.-Y. Liao.
2011. Estimates of life history parameters of the sharpspine skate, *Okamejei acutispina*, in the northeastern waters of Taiwan. Fish. Res. 108:258–267. Crossref

Kadri, H., S. Marouani, B. Saïdi, M. N. Bradai, M. Ghorbel, A. Bouaïn, and E. Morize.
2012. Age, growth and reproduction of *Raja miraletus* (Linnaeus, 1758) (Chondrichthyes: Rajidae) of the Gulf of Gabès (Tunisia, central Mediterranean Sea). Mar. Biol. Res. 8:388–396. Crossref

Kimura, D. K.
1980. Likelihood methods for the von Bertalanffy growth curve. Fish. Bull. 77:765–776.

Kume, G., K. Furumitsu, and A. Yamaguchi.
2008. Age, growth and age at sexual maturity of fan ray *Platyrhina sinensis* (Batoidea: Platyrhinidae) in Ariake Bay, Japan. Fish. Sci. 74:736–742. Crossref

Last, P., G. Naylor, B. Séret, W. White, M. Stehmann, and M. de Carvalho (eds.).
2016. Rays of the world, 790 p. CSIRO Publ., Clayton South, Australia.

Licandeo, R., and F. T. Cerna.
2007. Geographic variation in life-history traits of the endemic kite skate *Dipturus chilensis* (Batoidea: Rajidae), along its distribution in the fjords and channels of southern Chile. J. Fish Biol. 71:421–440. Crossref

Luer, C. A., and P. W. Gilbert.
1985. Mating behavior, egg deposition, incubation period, and hatching in the clearnose skate, *Raja eglanteria*. Environ. Biol. Fishes 13:161–171. Crossref

MEJ (Ministry of the Environment, Japan).
2017. Red list of threatened marine fishes in Japan, 6 p. Minist. Environ., Jpn., Tokyo, Japan. [In Japanese.] [Available from website, accessed February 2024.]

Palm, B. D., D. M. Koester, W. B. Driggers III, and J. A. Sulikowski.
2011. Seasonal variation in fecundity, egg case viability, gestation, and neonate size for little skates, *Leucoraja erinacea*, in the Gulf of Maine. Environ. Biol. Fishes 92:585–589. Crossref

Porcu, C., A. Bellodi, A. Cau, R. Cannas, M. F. Marongiu, A. Mulas, and M. C. Follesa.
2020. Uncommon biological patterns of a little known endemic Mediterranean skate, *Raja polystigma* (Risso, 1810). Reg. Stud. Mar. Sci. 34:101065. Crossref

Reis, M., and W. F. Figueira.
2020. Age, growth and reproductive biology of two endemic demersal bycatch elasmobranchs: *Trygonorrhina fasciata* and *Dentiraja australis* (Chondrichthyes: Rhinopristiformes, Rajiformes) from Eastern Australia. Zoologia 37:1–12. Crossref

Ricker, W. E.
1975. Computation and interpretation of biological statistics of fish populations. Bull. Fish. Res. Board Can. 191, 382 p.
1979. Growth rates and models. *In* Fish physiology, vol. 8 (W. S. Hoar, D. J. Randall, and J. R. Brett, eds.), p. 677–743. Acad. Press, New York.

Rigby, C. L., N. K. Dulvy, D. Derrick, Y. V. Dyldin, K. Herman, H. Ishihara, C.-H. Jeong, Y. Semba, S. Tanaka, I. V. Volvenko, et al.
2021. *Okamejei acutispina*. The IUCN Red List of Threatened Species 2021:e.T161636A124519140. [Available from website, accessed September 2022.]

Soto-López, K., R. I. Ochoa-Báez, F. Galván-Magaña, and M. C. Oddone.
2021. Reproductive biology of the rasptail skate *Rostroraja velezi* (Rajiformes: Rajidae). J. Fish Biol. 98:791–802. Crossref

Sulikowski, J. A., J. Kneebone, S. Elzey, J. Jurek, P. D. Danley, W. H. Howell, and P. C. W. Tsang.
2005. The reproductive cycle of the thorny skate (*Amblyraja radiata*) in the western Gulf of Maine. Fish. Bull. 103:536–543.

Sulikowski, J. A., S. B. Irvine, K. C. DeValerio, and J. K. Carlson.
2007. Age, growth and maturity of the roundel skate, *Raja texana*, from the Gulf of Mexico, USA. Mar. Freshw. Res. 58:41–53. Crossref

Yamada, U., M. Tokimura, H. Horikawa, and T. Nakabo.
2007. Fishes and fisheries of the East China and Yellow Seas, 1340 p. Tokai Univ. Press, Hadano, Japan. [In Japanese.]

Yamaguchi, A.
2002. On the sharks as fishery resources and aspects of their life histories. Aquabiology 24:401–408. [In Japanese.]

Yamaguchi, A., T. Taniuchi, and M. Shimizu.
1998. Geographic variation in growth of the starspotted dogfish *Mustelus manazo* from five localities in Japan and Taiwan. Fish. Sci. 64:732–739. Crossref

Yamamoto, K., and K. Nagasawa.
2015. Temporal changes in demersal fish assemblage structure in the East China Sea and the Yellow Sea. Nippon Suisan Gakkaishi 81:429–437. [In Japanese.] Crossref